

# Acoustoelectric Amplification in Lateral-Extensioal Composite Piezo-Silicon Resonant Cavities

Hakhamanesh Mansoorzare and Reza Abdolvand

Department of Electrical and Computer Engineering  
University of Central Florida

Orlando, USA  
hakha@knights.ucf.edu

**Abstract**—In this work, evidence for acoustoelectric (AE) amplification in lateral-extensioal thin-film piezoelectric-on-silicon (TPoS) resonant cavities for the first time is demonstrated. Due to the piezoelectric coupling, an evanescent electromagnetic wave is induced in the silicon (Si) layer that is a part of the resonant cavity, exchanging momentum with the carriers. Therefore, by injecting an electric current in this layer, the acoustic equivalent of Cherenkov radiation – AE amplification – can be realized. Such phenomenon is observed in a 1 GHz TPoS resonant cavity in which lateral field excitation is utilized to excite the acoustic wave.

**Keywords**—RF MEMS; piezoelectric; acoustoelectric amplification; resonator; composite resonant cavity;

## I. INTRODUCTION

Acoustoelectric (AE) effect, a bi-directional coupling between the acoustic waves (AW) and electron flow (i.e. current), fascinated a generation of physicists and engineers for decades during the 20<sup>th</sup> century. It was first observed by I. G. Shaposhnikov at 1941 that AW undergo attenuation when they propagate within an electron plasma and later a DC current was detected in conjunction with the AW [1-3]. A major implication of the AE phenomena was amplification of AW by means of an induced DC current in piezoelectric semiconductors such as cadmium sulfide [4, 5]. This momentum exchange requires that the electron drift velocity be higher than the AW velocity, however, such condition renders the AE amplification quite inefficient in common piezoelectric semiconductors due to their intrinsically low carrier mobility. Later, an alternative solution was suggested where they placed a high mobility semiconductor substrate adjacent to a good piezoelectric substrate such that the electric field associated with the AW traveling in the piezoelectric substrate penetrates into the semiconductor. As such, structures in which a semiconductor such as silicon (Si) is held in close proximity of a Lithium Niobate (LN) substrate where surface acoustic waves (SAW) are excited and detected were proposed, yielding limited success and efficiency due to the weak coupling between the two media and the fabrication complexities at the time [6, 7]. Nevertheless, SAW technology is considered an offshoot of early efforts in this field. The rise of gallium nitride (GaN) as a suitable candidate for high-electron mobility and power transistors, once more, invigorated research in AE interactions, leading to demonstration of gain in BAW GaN filters, for

instance [8]. In order to efficiently achieve the AE amplification, moderate carrier concentration for increasing the carrier mobility and reducing charge screening on one hand, and high electromechanical coupling on the other hand, are essential. By separating the piezoelectric and semiconductor properties from a single medium into two different media, these properties can be chosen and adjusted independently, improving the overall amplification performance. AE interactions have been previously observed in thin-film piezoelectric-on-silicon (TPoS) resonators through changing the surface carrier density at the semiconductor-piezoelectric interface that results in alteration of the insertion loss (IL) of such devices [9]. Here we show that AE gain can be realized in TPoS resonant devices by injecting a DC current through the Si layer in parallel with the direction of AW propagation. High-order lateral-extensioal TPoS resonant cavities operating at 1 GHz are chosen for proving the feasibility of this concept.

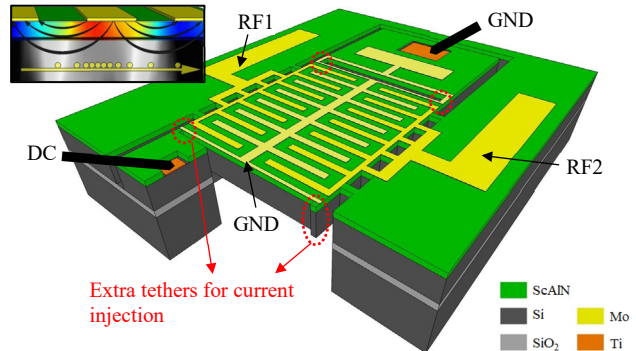


Fig. 1. Schematic of the device showing the electrode configuration for LFE as well as points of electrical contact to Si; inset visualizes AE interaction of piezoelectric field and electrons (yellow dots) in the device.

## II. DESIGN AND FABRICATION

A stack of 1  $\mu\text{m}$  (20%) scandium doped aluminum nitride ( $\text{Sc}_{0.2}\text{Al}_{0.8}\text{N}$ ) – having twice the electromechanical coupling of pure AlN [10] while being compatible with CMOS processing – sputtered on 2  $\mu\text{m}$  of lightly doped n-type Si (in the order of  $1\text{E}14 \text{ cm}^{-3}$ ) forms the acoustic cavity. The electrode configuration for this resonant device is modified compared to the previous typical design as the bottom metal is removed to facilitate penetration of electric fields between the piezoelectric and the semiconductor layers (Fig. 1). Instead, the top metal

layer is redesigned to enable lateral field excitation (LFE) of the harmonic lateral-extensional resonance mode at around 1 GHz. LFE is essential in the way that it ensures the electric field due to the piezoelectricity in ScAlN penetrates into the Si and exchanges momentum with the carriers within. Two extra pairs of tethers are added to the structure that form a current conduction path through the Si layer. Two access pads to Si are also opened up on the two ends of the cavity through which a DC current is injected in the Si. The DC contacts are isolated from the rest of the substrate to largely limit the current path through the resonant cavity.

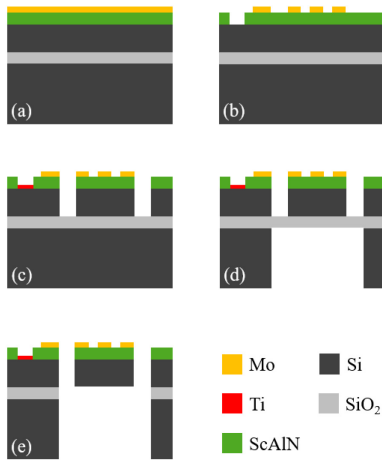


Fig. 2. Fabrication process flow showing (a) the initial stack (b) patterning top electrode and contacting the Si layer (c) etching the device layer (d) etching the backside (e) releasing the device.

The fabrication of the device, which is summarized in Fig. 2, starts with sputtering 1  $\mu\text{m}$  ScAlN on a silicon-on-insulator (SOI) substrate. The top metal layer, 100 nm molybdenum, is sputtered and patterned and contacts to the Si layer are formed by wet etching the piezoelectric layer in a heated TMAH based solution. A layer of Ti/Au is deposited on the Si contacts and the electrode pads to improve Ohmic contacts. Next, the boundary of the resonator is defined by etching the ScAlN and Si layer in chlorine based RIE/ICP and DRIE, respectively. Finally, the backside of the substrate is etched to the buried oxide (BOX) layer and the device is released by etching the BOX layer in buffered oxide etchant. The scanning electron micrograph (SEM) of the fabricated device is shown in Fig. 3.

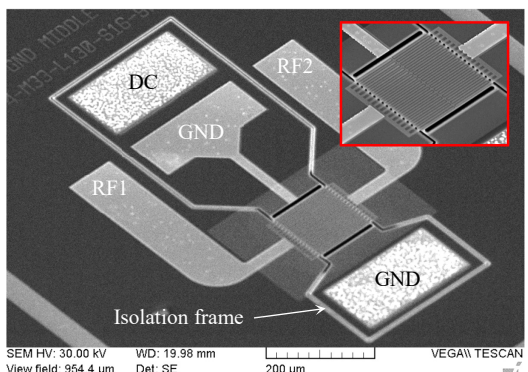


Fig. 3. SEM picture of the device studied herein for AE amplification

### III. EXPRESSION FOR THE AE AMPLIFICATION

In order to derive the expression for the AE interactions in composite resonant devices, the boundary conditions corresponding to the set of equations for the electric field and AW in both media are equated at their interface. This results in the dispersion equation for such structures [11] that can be modified and applied to the case of standing waves, as well [8]. Hence, the incremental loss/gain due to AE effect is written as:

$$\alpha_{AE} = K^2 G \omega \left( \frac{\eta-1}{(\eta-1)^2 + C^2 \left( 1 + \omega^2 / \omega_C \omega_D \right)^2} + \frac{\eta+1}{(\eta+1)^2 + C^2 \left( 1 + \omega^2 / \omega_C \omega_D \right)^2} \right) \quad (1)$$

Here  $K$  is the electromechanical coupling that is extracted from the admittance response of the resonator to be 0.4%,  $\eta$  is the ratio of the electron velocity ( $V_e$ ) to the AW velocity ( $V_a$ ),

$\omega_c = q\mu N / \epsilon_{Si}$  is the carrier relaxation frequency,  $\omega_D = qV_a^2 / k_B T \mu$  is the carrier diffusion frequency,  $\mu$  is the carrier mobility,  $G = \epsilon_{Si} d \omega_c [tgh(\beta d) / \beta d] / 2\epsilon_{ScAlN} V_a^2$ , and

$C = q\mu N d [tgh(\beta d) / \beta d] / \epsilon_{ScAlN} V_a$  where  $d$  is the thickness of the

Si layer,  $N$  is the free carrier concentration,  $\beta$  is the wave propagation constant,  $\epsilon_{Si}$  is the relative permittivity of Si,  $\epsilon_{ScAlN}$  is the relative permittivity of ScAlN,  $T$  is the temperature,  $k_B$  is Boltzmann constant, and  $q$  is the elementary charge. By separating the AE attenuation coefficient from the other sources of loss ( $\alpha_{\text{total}} = \alpha_{\text{other}} + \alpha_{AE}$ ) the insertion loss (IL) can be expressed in the form of:

$$IL(dB) = 20 \log_{10} \left( \frac{A_0 e^{\alpha_{\text{other}} + \alpha_{AE} (\cos(\omega t + \beta z) + \cos(\omega t - \beta z))}}{A_0 (\cos(\omega t + \beta z) + \cos(\omega t - \beta z))} \right) \quad (2)$$

Therefore, the term due to the AE loss/gain can be separated so that the right side of the equation (2) simplifies to sum of IL when no external voltage causes the electron drift and the electric gain due to the fast drifting electrons:

$$20 \log_{10} (\alpha_{AE}) + 20 \log_{10} \left( \frac{A_0 e^{\alpha_{\text{other}} (\cos(\omega t + \beta z) + \cos(\omega t - \beta z))}}{A_0 (\cos(\omega t + \beta z) + \cos(\omega t - \beta z))} \right) \quad (3)$$

### IV. MEASUREMENT RESULTS

While measuring the frequency response (i.e.  $S_{21}$ ) of the targeted device using a Rohde & Schwarz ZNB 8 network analyzer and a pair of Cascade Microtech GSG probes at room temperature in atmospheric pressure, a pair of DC probes are used to apply a DC voltage across the Si electrical contacts and the injected current is measured. The average IL of the device as a function of the applied voltages is plotted in Fig. 4 (solid blue line). By substituting the IL measured once no DC voltage is applied in the right-hand term of (3) and the electric gain resultant of the applied voltages which is calculated from (1) in the left-hand term, the expected IL is derived and plotted in Fig. 4 (dashed red line). At low injected current levels the measured and expected values are consistent, however, the larger the injected current gets, the more the measured IL deviates from what is theoretically expected; a 0.48 dB improvement in the IL

is expected upon passing 150  $\mu$ A current, while only a 0.23 dB enhancement is observed. Such discrepancy can be possibly attributed to the adverse effect of Joule heating in the device which reduces the electron mobility and higher interface trapped charges that screen the evanescent field in Si layer. The frequency response of the resonator as the current is increased is plotted in Fig. 5.

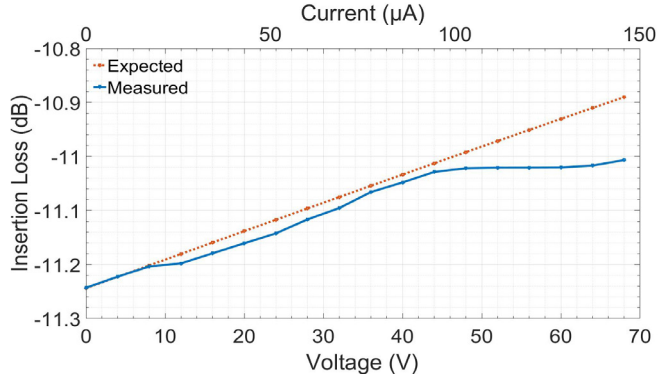


Fig. 4. Measured IL of the device and the expected values for 0-68 V (in 4 V increments) applied to the Si contacts of the device. The solid and dashed lines connecting the measurement datapoints are for visual guidance.

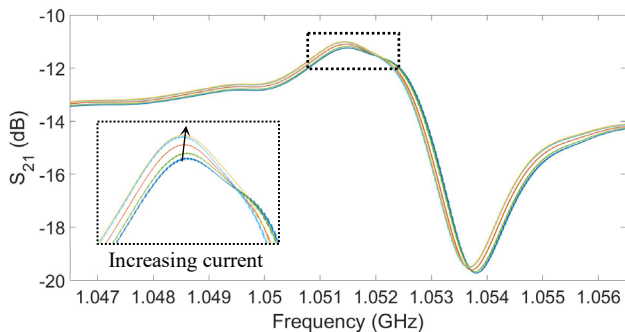


Fig. 5. Frequency response of the device for different injected currents from 0  $\mu$ A to 150  $\mu$ A showing improvements in the loss and  $Q$  as the current increases.

## V. CONCLUSIONS

Thin-film piezoelectric-on-silicon (TPoS) resonant cavities utilizing lateral field excitation (LFE) at 1 GHz were designed and fabricated for investigating the possibility of acoustoelectric (AE) amplification in such structures. LFE of the piezoelectric layer results in an evanescent field in the Si layer that exchanges momentum with the electrons within and once the electrons drift faster than the acoustic wave, by applying an electric field across the Si layer, AE amplification occurs. Good agreement between the measured and expected values was observed, especially at smaller applied voltages.

## ACKNOWLEDGMENT

This work was supported by the National Science Foundation (NSF) under award 1810143.

## REFERENCES

- [1] Y. V. Gulyaev, and F. S. Hickernell. "Acoustoelectronics: History, present state, and new ideas for a new era." In IEEE Ultrasonics Symposium, 2004 (Vol. 1, pp. 182-190). IEEE, 2004.
- [2] I. G. Shaposhnikov, JETP, 11, 332, 1941.
- [3] R. H. Parmenter, Phys. Rev., 89, 990, 1953.
- [4] Hutson, A. R., J. H. McFee, and D. L. White. "Ultrasonic amplification in CdS." Physical Review Letters 7.6 (1961): 237.
- [5] White, D. L. "Amplification of ultrasonic waves in piezoelectric semiconductors." Journal of Applied Physics 33.8 (1962): 2547-2554.
- [6] Gulyaev, Yu V., and V. I. Pustovoit. "Amplification of surface waves in semiconductors." Soviet Phys.—JETP 20 (1965): 1508-1509.
- [7] J. H. Collins, K. M. Lakin, C. F. Quate, and H. J. Shaw. "Amplification of acoustic surface waves with adjacent semiconductor and piezoelectric crystals." Applied Physics Letters 13.9 (1968): 314-316.
- [8] Gokhale, V. J., and M. Rais-Zadeh. "Phonon-electron interactions in piezoelectric semiconductor bulk acoustic wave resonators." Scientific reports 4 (2014): 5617.
- [9] H. Mansoorzadeh, R. Abdolvand, and H. Fatemi. "Investigation of Phonon-Carrier Interactions in Silicon-Based MEMS Resonators." 2018 IEEE International Frequency Control Symposium (IFCS). IEEE, 2018.
- [10] Wingqvist, G., et al. "Increased electromechanical coupling in  $W-Sc_xAl_{1-x}N$ ." Applied Physics Letters 97.11 (2010): 112902.
- [11] Kino, G. S., and T. M. Reeder. "A normal mode theory for the Rayleigh wave amplifier." IEEE Transactions on Electron Devices 18.10 (1971): 909-920.